

A Probabilistic Sensitivity Analysis of the Secondary Air System in Two-Spool Engines

*Dr. Salvatore Brischetto
Politecnico di Torino, Italy.*

Abstract

The present investigation aims at performing a probabilistic and sensitive analysis of a secondary air system for a two-spool engine. Through this analysis, the robustness of secondary air system could be gained and the most sensitive geometric parameters are found. Furthermore, the more restrictive mechanical tolerance could be demanded by the designer of secondary air system.

Indexed keywords: Computer Engineering, Advanced Computing, Technology, Open Access

Article History: Received: 18 April 2023 | Accepted: 27 June 2023 | Published: 07 July 2023

An in-house code called ASUS was developed for probabilistic and sensitive analysis, which is based on Monte Carlo Simulation method (MCS). The analysis model was based on the deterministic secondary air system network for a two-spool engine with take-off condition with all geometric parameters, including seals, gaps, holes and tubes. These parameters were normally distributed based on the real geometric tolerances to form the probabilistic inputs. The boundary condition was treated in two ways; one is constant while the other is normally distributed with an assumed change range $\pm 5\%$. Probabilistic and sensitive analyses were carried out on these two cases. Through the analyses, in both cases the rim seal after 1st rotor is sensitive to the mechanical tolerance and boundary change. Therefore, the special attention should be paid to this flow path.

INTRODUCTION

The secondary air system (SAS) could be “those airflows that do not directly contribute to the engine thrust”. The air that flows inside the SAS is generally bled from different compressor stages, either via slots in the outer casing, or at the inner through axial gaps or holes

in the drum. The air is then transferred either internally through a series of orifices and labyrinth finned seals, or externally via pipes outside the engine casing [1]. This air can represent more than 20 % of the engine core flow, and is therefore an important source of performance losses.

The SAS is very important to the operation of the engine, both for safety and performance reasons. The functions of SAS are the following [2]:

- Internal engine and accessory unit cooling;
- Control of axial pressure loading on the bearings;
- Prevention of hot gas ingestion into the turbine disc cavities;
- Isolation of the oil system;
- Control of turbine blade tip clearances;
- Engine anti-icing;
- Air supply for the aircraft services.

In the engine Secondary Air System is consisted of numerous numbers of flow elements, static elements and rotating components. The elements typically used are restrictors, seals and Dynamic head loss elements. Restrictors include holes or slots, rotating holes and nozzles. Common to these elements is that the flow is described by the gas dynamics flow function and a discharge coefficient Cd.

For traditional secondary air system design, all the geometric parameters and aerodynamic parameters is determined value for a given working condition, and the results of air system are also determined value. But in real operation, the geometric parameters are not the same, since each geometric size has its tolerance, and the geometry parametric parameters in air system flow path is different from engine to engine. On the other hand, the boundary condition like the pressure and temperature may also change.

Because of the importance of secondary air system to the safety and performance of engine, it is necessary to tell how the air system bears the input variability or uncertainty, and how confidence the outputs are. That is called the robustness of the secondary air system.

Probabilistic analysis is to determine how robust a system is. This type of analysis describes the variability of a system by analysing the outputs parameters after applying variation to certain inputs of that secondary air system. Typically the variability of system is described by standard deviation and confidence interval [3].

Another function of probabilistic analysis is input sensitivities calculation. That is, the causes of that variability are also quantified. Sometimes this information is just as important as the magnitude of the



output variability, since the output variability can be reduced if key sources of variability are known. For example, tolerances for the geometry of components can be relaxed if the output of the probabilistic analysis is found to be insensitive to them [3].

Previous studies in probabilistic secondary flow and heat transfer systems, even for the turbine air foil oxidation life predict. Base on the probabilistic results of air system, the downstream discipline would have the probabilistic inputs to do feather study. In this paper, some works done by the experts in this area are presented.

Ethan Stearns [3] perform probabilistic thermal analyses that include variability from the secondary flow system. A turbine one to two labyrinth seal was used as an example. Maximum metal temperature and temperature rise across the seal were the main outputs of interest. The maximum temperature was most sensitive to the air source temperature, and both the outputs were sensitive to the mass flow rate and heat transfer coefficient.

Vince Sidwell [4] analysed the variability of turbine airfoil oxidation life due to variability in the turbine cooling air portion of the auxiliary air system. Monte Carlo analysis is used to generate a distribution of the probability of oxidation failure for each of two airlines. The probabilistic distribution of failure times is compared to the field failure distributions of two airlines. Probabilistic results are similar to the field experience for the airline operating in a hotter environment.

David Cloud [5] documented a methodology for analysing turbofan secondary flow systems probabilistically. This type of analysis quantifies model outcomes when variation is applied to the inputs. It was used to find the variability in the total secondary flow and the axial loads on the high and low rotor bearings of a turbofan engine. The sensitivity of output parameters to input variability was also identified. Another application to a small model of the station 2.5 bleed system was also given, showing that the source pressure variability was the cause of almost all of the variability in bleed flow.

Adam Cooke [6] compared two methods of uncertainty analysis, Monte Carlo simulation method and a Taylor series uncertainty propagation method, for the calculation of local disc to air heat fluxes and corresponding heat transfer coefficients for a free disc test case having a turbulent flow regime. Monte Carlo method is better suited to this calculation.

Stefan Brack [7] presented the methodology Latin Hypercube Sampling (LHS) and the results of probabilistic analysis of the secondary air system. The effects of the uncertainty in geometrical quantities and engine performance parameters on the cooling mass

flow, the axial bearing load and possible hot gas ingestion in the secondary air system of a three-stage high-speed low-pressure turbine were investigated at one engine condition - take-off. A sensitivity analysis was performed detecting the main sources of the uncertainty for every output variable individually.

The previous analysis is based on part of secondary air system, it also necessary to carry out probabilistic and sensitive analysis on the whole system.

A code called ASUS (Air System Uncertainty and Sensitive) was developed to carry out the analysis in this paper. The calculation of air system network is based on another in-house code Flownet. The analysis carried out on a whole secondary air system for a two-spool turbofan engine. The main concerned is about the uncertainty of main outputs, like air flow rate, sealing pressure, axial load, etc. And find out the sensitive sources to these outputs.

ANALYTICAL MODEL

Deterministic aerodynamic

network

Fig 1 to Fig 3 shows a typical two-spool engine and the secondary flow path. The engine has two rotors, low pressure (LP) rotor and high pressure (HP) rotor. The air bleed from high pressure compressor (HPC) 1st stage is used to seal the three bearing chamber, and the air from 4th stage used to cool the low pressure turbine (LPT) and the rim seal after 2nd rotor. The HPC 7th bleed from two position, one from the tip to cool the 2nd vane and supply the rim seal air for the rim seal location after high pressure turbine (HPT) 1st blade and before 2nd blade. The other HPC 7th bleed from the hub, pass through the vortex reducer and the holes to cool the 2nd blade. The HPC 10th hub bleed air and the combustor inner annulus air is used to cool the NGV and HPT 1st blade, also supply the rim seal flow before the HPT 1st blade.

To adjust the axial load for LP rotor, an adjust chamber designed after the LPT shaft.

1-D network was built to calculate the air system. All parameters are the design value in take-off condition. The calculation is carried out using the in-house code Flownet.

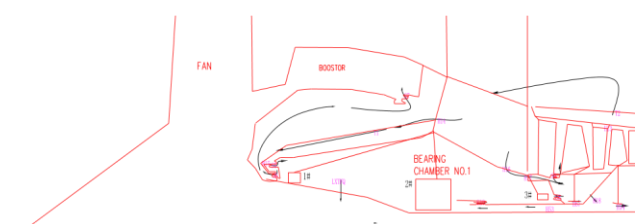


Fig1 Engine model and air flow path (front)

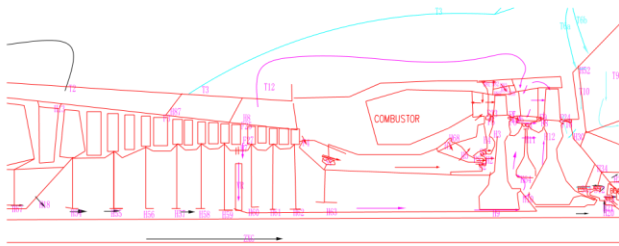


Fig 2 Engine model and air flow path (middle)

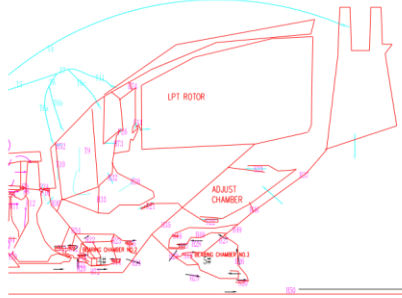


Fig3 Engine model and air flow path (rear)

Probabilistic system

For the probabilistic analysis in this paper, the secondary air system use the same network as deterministic analysis, while the geometry and aerodynamic parameters could be probabilistic.

The geometric parameters which are considered to be probabilistic distributed is the hole, tubes, seal clearance, etc. The position of geometric parameter is shown in Fig1 to Fig3.

OVERVIEW OF METHODOLOGY

A code called ASUS (Air System Uncertainty and Sensitive) was developed to carry out the analysis in this paper. The method used in this code is Monte Carlo Simulation (MCS). An overview of the principle is shown in Fig4.

Three steps to do this analysis. First the random distributions of input parameters are generated, then formed into input files. The input parameters may be geometric or aerodynamic. For the geometric inputs the random distribution is normal distribution.

The second step is to carry out n_s times 1D network calculation to get output files. The third step is to analyze the robustness of the air system, by analysis of output parameters from output files, each result parameter has its distribution.

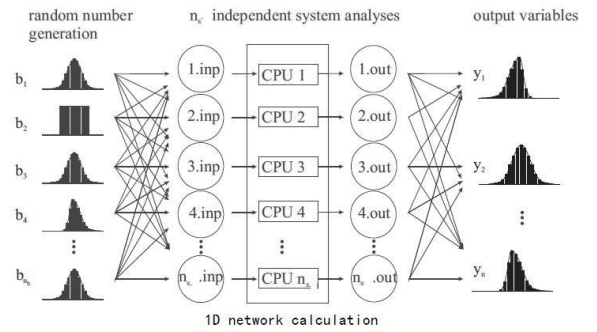


Fig4 Principle of the Monte Carlo Simulation [8]

The linear correlation coefficient is introduced in this study. The definition of linear correlation coefficient r is equation (1). This coefficient built the relationship between the input variations to their responded outputs; make it possible to identify most sensitive parameter.

$$r = \frac{\sum_{i=1}^n (b_i - \bar{b})(y_i - \bar{y})}{\sqrt{\sum_{i=1}^n (b_i - \bar{b})^2 \sum_{i=1}^n (y_i - \bar{y})^2}} \quad (1)$$

Where r is the linear correlation coefficient, b_i is the random distributed input element, y_i is the output parameter, n is the sample number.

STOCHASTIC INPUT VARIABLES

Geometric input variables

The geometric input variables are the mechanical tolerance in the geometric size. The types of inputs including clearance of seal and rim seal or gaps, diameter of holes or tubes. The location of geometric parameters is shown in Fig1 to Fig3. The symbol 'S' represent seal, and 'H' is hole, 'F' is gap, 'T' is tube.

Typical geometric variables range by the real mechanical tolerance is shown in Table 1. It is obviously that the distribution range for seal is much bigger than that of holes and tubes. For the seal the changing range of clearance may up to $\pm 15\%$ while the hole and tube diameter effect is just $\pm 1\%$. This kind of relative difference may result in different output change which will be discussed in the result part of this paper. An example of geometric variable distribution is shown in Fig5.

Table1 Typical geometric variables

Location	μ	σ	$\mu - 3\sigma$	$\mu + 3\sigma$
S1	1	0.028	0.92	1.08
S4	1	0.016	0.95	1.05
S5	1	0.049	0.85	1.15
H13	1	0.003	0.99	1.01
T1	1	0.003	0.99	1.01

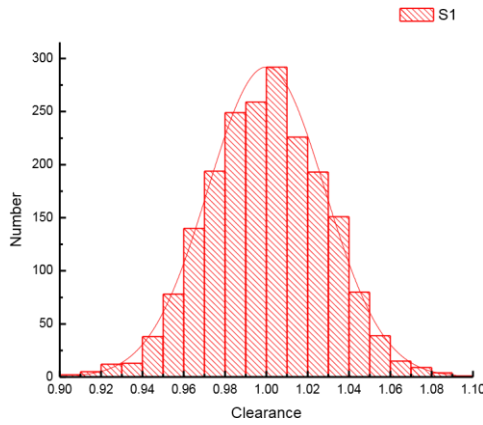


Fig 5 Distribution of S1

Boundary conditions

Two types of boundary conditions were considered in this paper. First the aerodynamic boundary conditions assumed to be determined and all probabilistic input files use the same boundary condition.

Second case, the boundary condition including pressure and temperature changed in some distribution. Since the aerodynamic could not supply distribution of the pressure in the HPC or HPT, in this paper we assume that the boundary pressure and temperature is normal distribution, and the change range assumed to be $\pm 5\%$.

Fig6 shows the distribution of pressure with $\pm 5\%$ range distribution.

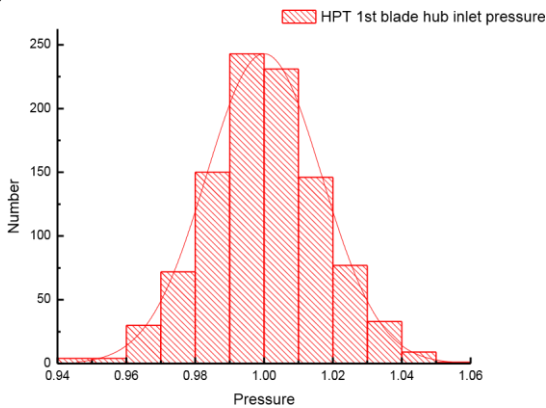


Fig6 HPT 1st blade hub inlet pressure

RESULTS AND DISCUSSION

Probabilistic analysis

Probabilistic analysis for bleed air flow is shown in table 2. All the flow rates are divided by the mean value. An example of flow rate distribution is shown in Fig8, all flow rates are normal distribution.

The results show 99.7% possibility range ($\pm 3\sigma$) for each flow rate. For HPC 10th hub, the accuracy is $\pm 7.1\%$. All the other flow rates have smaller range from $\pm 0.3\%$

to $\pm 2.2\%$. The flow rate with smallest change is the HPC 7th stage hub flow.

The range in table 2 show the effects of tolerance of geometry parameters on the bleed air flow rates. The $\pm 3\sigma$ probabilistic range is also the ‘tolerance’ of bleed air flow.

The reason why the HPC 7th stage hub flow has the smallest range is because of the flow path. In the 7th stage hub flow path there is no seal, only holes and vortex reducer. And the tolerance for hole is typically $\pm 0.1\text{mm}$ in diameter which result in little change in area. While for the seals, the tolerance of 0.05mm in clearance may result in 30% change in area for a seal with 0.15 mm designed clearance.

The case only considerate the tolerance of parameters has the flow rate changes less than 8%.

Table2 Probabilistic of bleed air flow

Location	μ	σ	$\mu-3\sigma$	$\mu+3\sigma$
HPC 1st stage	1	0.007	0.978	1.022
HPC 4th stage	1	0.002	0.993	1.007
HPC 7th stage tip	1	0.003	0.990	1.009
HPC 7th stage hub	1	0.001	0.997	1.003
Combustor inner annulus	1	0.006	0.982	1.018
HPC 10th hub	1	0.024	0.929	1.071

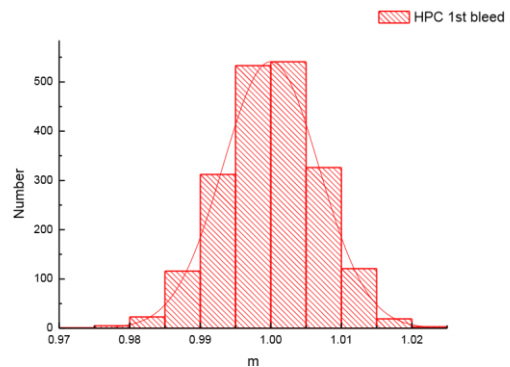


Fig7 HPC 1st bleeds

Table 3 shows probabilistic of air flow for some key flow paths. The distribution range for the rim seal flow after HPT 1st blade is $\pm 13\%$, which is much bigger than the HPC 7th bleed air flow. The distribution is shown in Fig15. This place will be further discussed in the sensitive analysis. For the 1st blade cooling flow, the distribution is only $\pm 1\%$ and the influence is quite small.

Table 3 Air flow in key flow path

Location	μ	σ	$\mu-3\sigma$	$\mu+3\sigma$
Rim seal aft 1st Rotor	1	0.044	0.868	1.132
Rim seal before 1st Rotor	1	0.017	0.949	1.051
Rim seal aft 2nd Rotor	1	0.012	0.963	1.037
2nd blade cooling flow	1	0.001	0.997	1.003

1st blade cooling flow 1 0.004 0.988 1.012

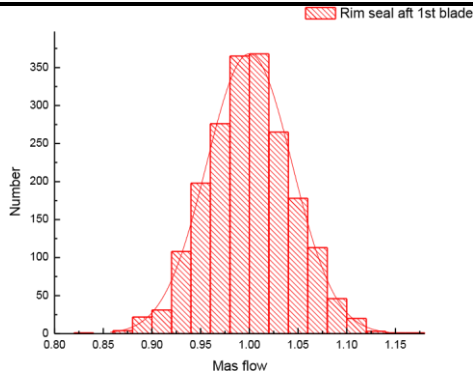


Fig8 Air flow distribution for rim seal aft 1st blade

Pressure difference for bearing sealing is shown in table 4. The biggest change is $\pm 12\%$. The distribution of Seal pressure difference for 1# front is shown in Fig9.

Table4 Pressure difference for bearing sealing

Location	μ	σ	$\mu-3\sigma$	$\mu+3\sigma$
1#front	1	0.040	0.88	1.12
2#front	1	0.020	0.94	1.06
3#rear	1	0.017	0.95	1.05
4#front	1	0.042	0.88	1.12
4#rear	1	0.041	0.88	1.12
5#front	1	0.031	0.91	1.09

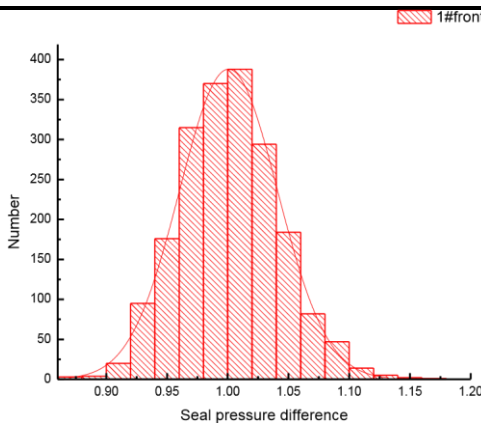


Fig9 Seal pressure difference for 1# front

Table 5 gives the distribution of rotor axial load for both low pressure rotor and high pressure rotor. The confidence ranges are $\pm 9\%$ and $\pm 7\%$. And the distribution of axial load is shown in Fig10.

Table5 Rotor axial load

Location	$\mu-3\sigma$	μ	$\mu+3\sigma$	
Low Pressure Rotor	1	0.030	0.91	1.09
High Pressure Rotor	1	0.024	0.93	1.07

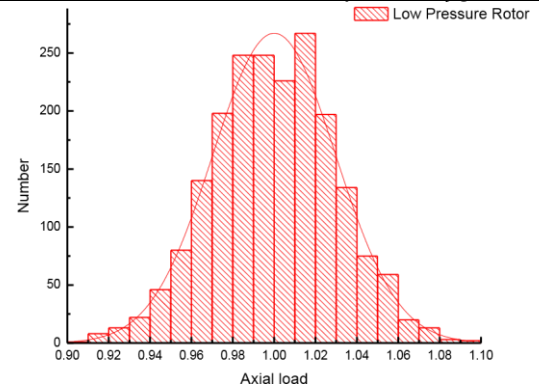


Fig10 Axial load for Low Pressure Rotor

Sensitive analysis

Sensitive analysis carried for all results against the geometry parameters, and a matrix of linear correlation coefficients available to analysis either which parameter has more impact on chosen result or which result is more impacted by the chosen parameter. In this paper, we'd like to choose the first eyesight and try to find the sensitive parameter for chosen result.

Since there are too many results to analysis, some examples were chosen in this paper. We choose HPC 10th bleed air, air flow distribution for rim seal aft 1st blade, axial load for Low Pressure Rotor, pressure difference for 4# bearing rear seal as the example.

Fig11 shows the distribution of linear correlation coefficient for the 10th bleed air. The top 3 linear coefficient and related parameters are shown in table 6. For the 10th bleed air, the most sensitive parameter is the CDP seal S1, and the coefficient near 1.0. The scatter figure Fig 12 is nearly straight line. With the smaller coefficient of F4, the 10th bleed air does sensitive to its clearance, as is shown in Fig13.

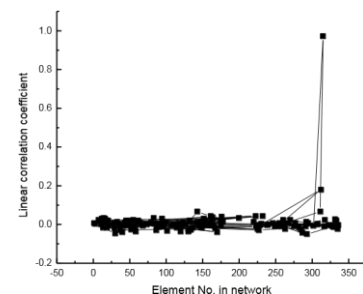


**Fig11 Linear correlation coefficients for the
10th bleed air**

**Table6 Top 3 sensitive parameters for 10th bleed
air**

Parameters	Linear coefficient
CDP seal S1	0.973
Bleed gap F4	0.181
Seal S2	0.067

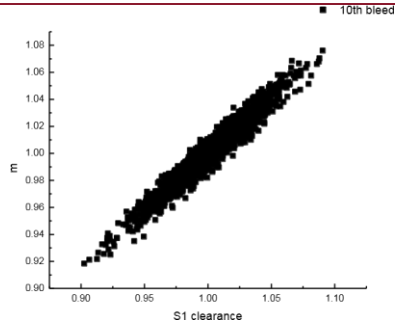


Fig12 10th bleeds mass flow vs. S1 clearance

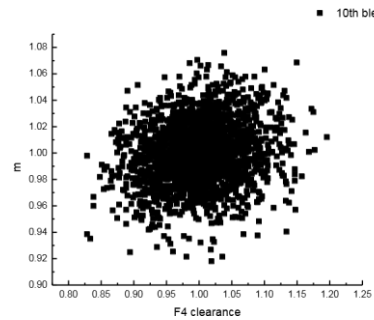


Fig13 10th bleeds mass flow vs. F4 clearance

Similar analysis carried out for the combustor inner annulus air, which is critical to the supply of cooling air to the 1st blade. The result shows the most sensitive element is the pre-swirl nozzle, as is seen in table7 and Fig14.

Table7 Top 2 sensitive parameters for combustor inner annulus air

Parameters	Linear coefficient
Pre-swirl nozzle PS	0.998
inner annulus hole H1	0.057

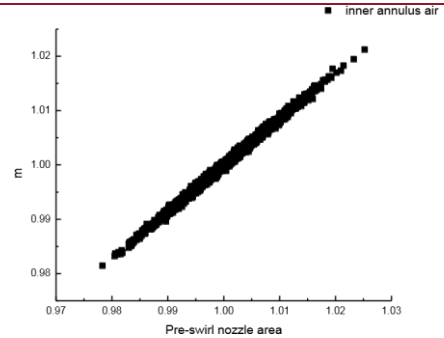


Fig14 Combustor inner annulus air vs. pre-swirl nozzle area

There are two main sensitive sources for rim seal flow aft 1st blade, as is shown in Table8. The inter stage seal S4 has negative effect while the supply hole H6 has positive effect. The effect of S4 is shown in Fig15.

Table8 Top 2 sensitive parameters for rim seal aft 1st blade

Parameters	Linear coefficient
Inter stage seal S4	-0.687
Supply hole H6	0.666

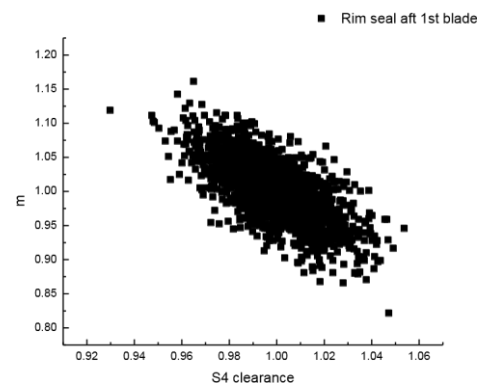


Fig15 Rim seal aft 1st blade vs. S4 clearance

Table9and table10 show the sensitive parameters for seal pressure difference. Result shows the most sensitive parameter is the bearing seal. The effect of S5 and S13 are shown in Fig16 and Fig17.



Table9 Top 4 sensitive parameters for 1# front seal pressure difference

Parameters	Linear coefficient
1#front seal S5	-0.853
1#front chamber seal S6	-0.416
3#rear seal S8	-0.225
2#front seal S10	-0.140

Table10 Top 4 sensitive parameters for 4# front seal pressure difference

Parameters	Linear coefficient
4#front seal S13	-0.680
4#rear seal S14	-0.564
3#rear seal S8	-0.249
1#front seal S5	-0.238
5#front seal S18	-0.204
2#front seal S10	-0.196

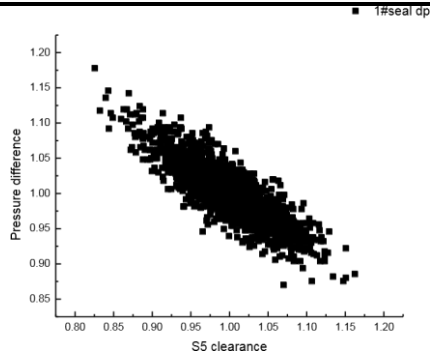


Fig16 1#front seal pressure difference vs. S5 clearance

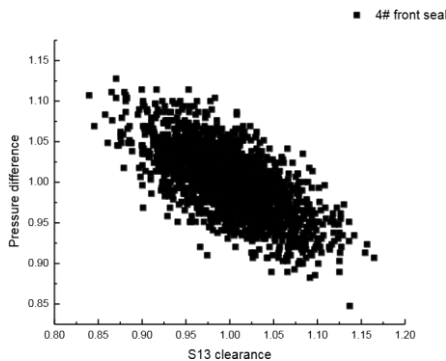


Fig17 4#front seal pressure difference vs. S13 clearance

Sensitive parameters for axial load are shown in table11 and table12. For the HP rotor, the bleed gap F4 has the most positive effect, and the CDP seal S1 has negative effect. Since the chamber between F4 and S1 is the main source of HP rotor axial load, the sensitive result is agreed with common sense.

For the LP axial load, the most sensitive two parameters are the top and bottom seal for the adjust chamber, which is also reasonable.

Table11 Top 3 sensitive parameters for HP axial load

Parameters	Linear coefficient
Bleed gap F4	0.77
CDP seal S1	-0.46
Pre-swirl nozzle PS	-0.36

Table12 Top 3 sensitive parameters for LP axial load

Parameters	Linear coefficient
Adjust chamber top seal S23	-0.83
Adjust chamber bottom seal S22	-0.52
Booster drum exit seal S7	-0.16

±5% change in boundary condition case

In the second case of analysis the boundary condition of air system network assumed to have ±5% change range both pressure and temperature, and the distributions are also normal distribution.

The probabilistic results discussed including bleed mass flow, key flow path mass flow, seal DP, axial load, are presented in table13 to table16. The changing range for these results is much bigger than the case with determined boundary conditions. Especially for the rim seal aft 1st rotor and axial load for high pressure rotor, the change range is ± 73% and ±58% respectively, while for the case with no boundary change; the value is only ±13% and ±7%. For this case the rim seal flow after 1st blade is likely to be not sufficient and hot gas may goes into the chamber.

For the rim seal before 1st rotor, the range becomes ± 29% which is 5 times of the case with determined boundary.

These results show the dramatic effect of the boundary conditions, but based on the assumption that

JCE

the boundary condition change range $\pm 5\%$, while in real gas turbine, the change range may not be that big. However, the results show the rim seal flow before and after 1st blade and HP axial load are more sensitive to the boundary condition change than other results.

Table13 Bleed mass flow with probabilistic boundary

Location	μ	σ	$\mu-3\sigma$	$\mu+3\sigma$
HPC 1st stage	1	0.027	0.919	1.081
HPC 4th stage	1	0.025	0.926	1.074
HPC 7th stage tip	1	0.031	0.907	1.093
HPC 7th stage hub	1	0.021	0.936	1.064
Combustor inner annulus	1	0.048	0.855	1.145
HPC 10th hub	1	0.039	0.882	1.118

Table14 Seal DP with probabilistic boundary

Location	μ	σ	$\mu-3\sigma$	$\mu+3\sigma$
1#front	1	0.048	0.86	1.14
2#front	1	0.031	0.91	1.09
3#rear	1	0.030	0.91	1.09
4#front	1	0.045	0.86	1.14
4#rear	1	0.038	0.89	1.11
5#front	1	0.036	0.89	1.11

Table15 Key flow path mass flow with probabilistic boundary μ

Location	μ	σ	$\mu-3\sigma$	$\mu+3\sigma$
Rim seal aft 1st Rotor	1	0.096	0.77	1.29
Rim seal aft 2nd Rotor	1	0.055	0.84	1.16
2nd blade cooling flow	1	0.018	0.95	1.05
1st blade cooling flow	1	0.017	0.95	1.05

Table16 Axial load with probabilistic boundary

Location	μ	σ	$\mu-3\sigma$	$\mu+3\sigma$
Low Pressure Rotor	1	0.056	0.83	1.17
High Pressure Rotor	1	0.194	0.42	1.58

Table17 shows the sensitive parameters for the rim seal mass flow after 1st rotor. The top 2 parameter become the bleed point pressure and the exit pressure, while the geometry parameter effect is overshadowed by the effect of pressure change. Rim seal mass flow aft 1st Rotor with HPT

A Probabilistic Sensitivity Analysis of the Secondary...

1st blade hub exit pressure is shown in Fig18.

Table17 Sensitive parameters for rim seal mass flow aft 1st Rotor

Parameters	Linear coefficient
HPT 1st blade hub exit pressure	-0.721
HPC 7th tip pressure	0.689
Supply hole H6	0.128
Inter stage seal S4	-0.092

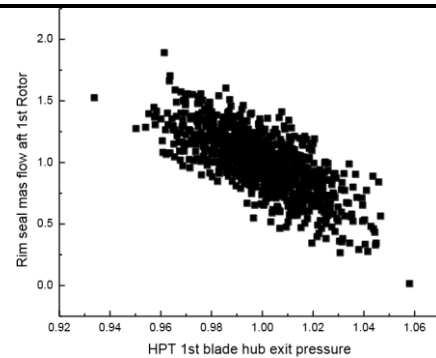


Fig18 rim seal mass flow aft 1st Rotor vs. HPT 1st blade hub exit pressure

For the HP axial load, the sensitive parameters are also inlet and exit pressure in network. See table18 and Fig19.

Table18 Sensitive parameters for HP axial load

Parameters	Linear coefficient
HPT 1st blade hub inlet pressure	-0.716
HPC 10th blade hub exit pressure	0.617
HPT 2nd blade hub exit pressure	0.236
combustor inner annulus pressure	-0.207

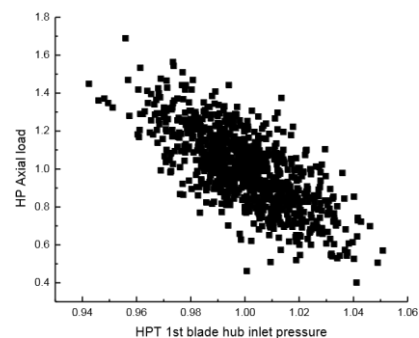


Fig19 HP axial load vs. HPT 1st blade hub inlet pressure

CONCLUSIONS

An in-house code of probabilistic and sensitive analysis, ASUS, was developed based on the MCS method and a 1D network, solved by the in-house code Flownet.

The probabilistic and sensitive analysis carried out for a two-spool turbofan engine, with two kind of case. One case considered the geometric tolerance for geometric parameters and the other was assumed to be $\pm 5\%$ change based on the first case. Both case analysed the confidence interval of results and the sensitive sources of input changes.

The case based on fixed boundary showed the uncertainty for mass flow is less than $\pm 8\%$; the axial load uncertainty is under $\pm 9\%$; the bearing sealing pressure difference uncertainty is under $\pm 12\%$; the uncertainty of rim seal flow after 1st blade is $\pm 13\%$, which is the biggest value in case 1.

The probabilistic result in case 1 study also showed that the flow path with more seal may have larger uncertainty than other flow path, since the mechanical tolerance had larger change in area for seal or gap than that of holes or tubes.

The sensitive analysis with case 1 showed the code is able to pick the sensitive parameters by linear correlation coefficients. Results were accord with common sense.

The case with $\pm 5\%$ change range showed the rim seal after 1st rotor, rim seal before 1st rotor and HP axial load were more sensitive to boundary change, and the change range become $\pm 73\%$, 29% , $\pm 58\%$ respectively compared with the value $\pm 13\%$, 5% , $\pm 7\%$ of the case with no boundary change.

The sensitive analysis showed the change $\pm 5\%$ in boundary could overshadow the influence of mechanical tolerance. To study the effect of mechanical tolerance and to find the key geometric size, it is better to have fixed boundary conditions.

In both cases, the rim seal after 1st rotor is sensitive to the mechanical tolerance and boundary change; special attention should be paid to this flow path.

REFERENCE

- [1] Philip P. Walsh, Paul Fletcher. Gas Turbine Performance, Second edition [M]. UK: Blackwell Science Ltd, 2004
- [2] Chew, J. W. "Developments in turbo machinery internal air systems", Proceedings of the Institution of Mechanical Engineers, Part C [J]. Journal of Mechanical Engineering Science, 2009, Vol. 223, No. 1, p. 189-234.
- [3] Ethan Stearns, Dave Cloud, et al. Probabilistic thermal analysis of gas turbine internal hardware[R], ASME Paper, 2006-GT-90881, 2006
- [4] Vince Sidwell, David Darmofal, et al. probabilistic analysis of a turbine cooling air supply system: the effect on airfoil oxidation life[R], ASME Paper, 2003-GT-38119, 2003
- [5] David Cloud, Ethan Stearns, et al. Probabilistic analysis of a turbofan secondary flow system[R]. ASME Paper 2004-GT-53197, 2004
- [6] Adam Cooke, Peter Childs, Christopher Long, et al. Investigation into the effect of uncertainty in thermal properties on turbo machinery disc heat transfer using both a monte carlo simulation Technique and a Taylor series uncertainty propagation method[R], ASME Paper, 2007-GT-27573, 2007
- [7] Stefan Brack, Yannick Muller, et al. Probabilistic analysis of the secondary air system of a low-pressure turbine[R], 2014-GT-26184, 2014
- [8] Thomas Bischoff, Matthias Voigt, and Ed Chehab, et al. Probabilistic analysis of stationary gas turbine secondary air Systems[R], 2006-GT-90261, 2006